Discrete and Stereospecific Oligomers Prepared by Sequential and Alternating Single Unit Monomer Insertion

Zixuan Huang,[a] Benjamin B. Noble,[b] Nathaniel Corrigan,[a] Yingying Chu,[a] Kotaro Satoh,[c] Donald Thomas,[d] Craig J. Hawker,[e] Graeme Moad,[f] Masami Kamigaito,[c] Michelle L. Coote,[b]* Cyrille Boyer,[a]* and Jiangtao Xu[a]*

[a]Centre for Advanced Macromolecular Design and Australian Centre for NanoMedicine, School of Chemical Engineering, UNSW Sydney, NSW 2052, Australia

[b]ARC Centre of Excellence for Electromaterials Science, Research School of Chemistry, Australian National University, Canberra, ACT 2601, Australia

[c]Department of Molecular and Macromolecular Chemistry, Graduate School of Engineering, Nagoya University, Furo-cho, Chikusa-ku, Nagoya 464-8603, Japan

[d]Nuclear Magnetic Resonance Facility, Mark Wainwright Analytical Centre, UNSW Sydney, NSW 2052, Australia

[e]Materials Research Laboratory and Departments of Materials, Chemistry and Biochemistry, University of California, Santa Barbara, California 93106, United States

[f]CSIRO Manufacturing Bag 10, Clayton South, VIC 3169, Australia

ABSTRACT

Natural biopolymers, such as DNA and proteins, have uniform microstructures with defined molecular weight, precise monomer sequence and stereoregularity along the polymer main chain that affords them unique biological functions. To reproduce these structurally perfect polymers and understand the mechanism of specific functions through chemical approaches, researchers have proposed using synthetic polymers as an alternative due to their broad chemical diversity and relatively simple manipulation. We reported a new methodology to prepare sequence-controlled and stereospecific oligomers using alternating radical chain growth and sequential photoinduced RAFT single unit monomer insertion (Photo-RAFT SUMI). Two families of cyclic monomers, indene and *N*-substituted maleimide, can be inserted into RAFT agents alternatively, one unit at a time, allowing monomer sequence to be controlled through sequential and alternating monomer addition. Meanwhile, the stereochemistry of cyclic monomer insertion into the RAFT agents is *trans*- selective along the main chains due to steric hindrance from the repeating monomer units. All investigated cyclic monomers follow the same trend, but acyclic monomers prefer mixed *cis*- and *trans*-configurational insertion into RAFT agents.

INTRODUCTION

Natural polymers, such as nucleic acids and proteins, are the basic structural components of living matter, which participate in the construction of genes, cells, and tissues. These bioorganic macromolecules possess precise monomer sequences and monomer chirality in their chemical structures which contributes to tuning inter- and intracellular interaction, defining functional interfaces, and storing chemical or genetic information.[1-4] The monomer sequence along these polymer chains defines the primary structure of macromolecules and the position of specific functionalities, while the monomer chirality is responsible for the chemical configuration of molecular segments which will principally contribute to the helical formation and spatial arrangement of macromolecular assemblies. For most naturally-occurring polymers, helical structures are essential for exerting their sophisticated functions in nature.[5-7]

Reproducing the chemical structures of these functional biomacromolecules and mimicking their natural processes to understand the underlying mechanisms has been a great challenge for more than half a century. There has been limited success, and for instance, scientists have duplicated these structurally perfect polymers from their natural monomers (nucleotides and amino acids) using chemical approaches, such as solid-phase peptide synthesis and oligonucleotide synthesis, to create new macromolecules for a range of biomedical and pharmacological applications.[8-10] However, problems still remain in these systems with a limited monomer and reaction setup scope restricting the large scale production and innovation of diverse polymer structures. Additionally, such synthetically assembled polymers based on natural monomers have the issue of in vitro and in vivo biostability, which limits the biomedical applicability due to adverse enzymatic degradation.[11] Taking these concerns into account, researchers have proposed using synthetic polymers derived from non-natural monomers (e.g. vinyl monomers from petroleum industry) with defined monomer sequence and chirality as an alternative, due to their broad chemical diversity, relatively simple manipulation, and improved biostability.[12] Most importantly, such polymers have the potential to open new opportunities for the development of advanced materials for data storage,[13-16] catalysis[17-18] and drug delivery.[19-21]

Various strategies have been proposed for regulating monomer sequence and chain length of synthetic polymers, including condensation chain polymerization,[22] alternating radical polymerization,[23-29] anionic polymerization,[30-31] ring-opening or cross metathesis polymerization,[32-34] atom transfer radical addition (ATRA),[24-25, 35-37] iterative exponential growth,[38-43] single unit monomer insertion[12, 44-50] and various organic coupling, condensation or “click” addition reactions.[19, 51-65] Separation techniques, which include automated flash chromatography[66-68] and preparative recycling size exclusion chromatography,[48, 69] have also been developed to isolate discrete oligomers from synthetically derived oligomer mixtures. Recent developments

have been summarized in comprehensive review articles.[70-73]

Compared to sequence control, stereoselectivity in the polymerization of non-natural monomers is far more challenging and has received relatively little attention. Since the first discovery of synthetic isotactic polypropylene in 1955,[74] the development of polymerization techniques capable of controlling the stereochemistry of vinyl polymers has generated considerable interest in polymer science, as the stereoregularity significantly affects the physical and chemical properties of synthetic polymers.[7, 75-77] To mimic the natural precision of biopolymers, both sequence- and stereo-controls are vital, which requires monodisperse or uniform synthetic polymers. In recent elegant reports by Johnson's group,[41, 78-79] exponential chain growth of chiral monomers (*R* and *S* configurations) can be incorporated into discrete polymers with different block sequences using "click" chemistry. Hawker and Qiao's work employed column chromatography to separate discrete and monodisperse isotactic and syndiotactic poly(methyl methacrylate) (PMMA) with defined monomer units, which were used to investigate the triple helix formation of such polymers.[68]

Recently, our group prepared discrete oligomers with monodisperse character and defined monomer sequences using single unit monomer insertion (SUMI) into thiocarbonylthio compounds in high yield (up to 95% isolated yield).[46, 49, 80] The synthesis of these discrete oligomers was based on the principle of selective photoactivation of SUMI adducts, in which the increased C-S bond dissociation energy of the SUMI adduct was used to suppress reactivation and multiple monomer insertions, which would reduce product purity and yield. As such, a major challenge is the selection of appropriate monomer and chain transfer combinations that meet these activation selectivity criteria. As a result, the monomer pool for subsequent SUMI is reduced which increases the difficulty in preparing longer oligomers and in controlling oligomer structures.

In this article, these previous SUMI procedures have been significantly improved to allow for preparation of discrete oligomers and "infinite" chain growth through a sequential and alternating process. This new protocol relies on an alternating monomer strategy in which two families of monomers, i.e., indene (Ind) and maleimide, are able to be alternatively inserted into the oligomers but not to homopolymerize. The reaction kinetics for one pair of alternating reactions are much easier to study in this process, while repetition of the alternating process provides a facile method for increasing chain length while maintaining specificity. Most importantly, the selected monomer families can be adapted to carry diverse functionality, for instance, a plethora of maleimide monomers are available through substitution at the nitrogen position. As a result, the currently disclosed strategy allows the monomer sequence and position of functionality to be tuned along the polymer chain.

Most significantly, these cyclic monomers insert in a stereospecific manner to form *trans*- linkages along

the polymer backbone (**Figure 1**), even though the SUMI process is a radical chain growth mechanism, which generally has less stereoselectivity. This is the first report of investigating stereochemistry of discrete polymers prepared by SUMI processes. This SUMI method provides the opportunity to engineer stereochemistry of every monomer through organic reactions during each cycle of insertion at a molecular level. The discrete oligomers formed herein can be expanded to access a library of functional building blocks with designed molecular chirality, enabling high order polymers to be prepared with sequence-specific positioning of functionalities and chirality, and thus to rationally design interaction capabilities by mimicking biological systems.

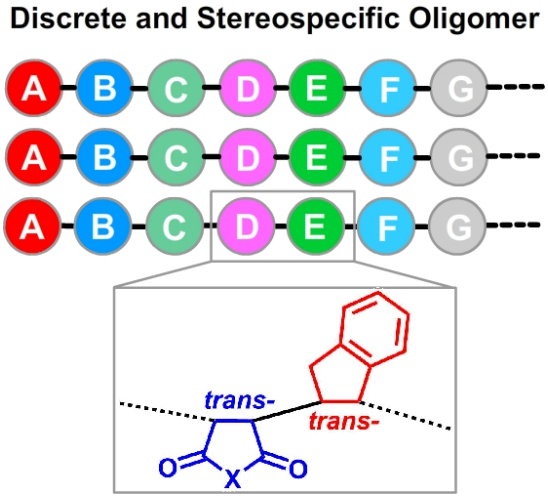

Figure 1. Precise structure of discrete and stereospecific oligomers. X denotes functional substitution of the maleic or maleimide monomer unit.

In this article, we investigate the mechanism of sequential and alternating photo-RAFT SUMI and introduce the general criteria for screening monomers, RAFT agents and reaction conditions. Next, two model pentamers with alternating Ind/maleimide monomers with diverse functionalities, were synthesized to showcase the efficiency, versatility and robustness of this method. Interestingly, these cyclic monomers have specific stereochemistry when inserted into the polymer chain, which gives only *trans*- configurations due to steric hindrance, regardless of the reaction conditions, monomer families and functionalities. In the last part of this article, we discuss the stereospecificity of the cyclic monomers inserted into various RAFT agents with chiral and non-chiral R (leaving) groups. 1D/2D NMR, XRD and modeling simulations are employed to verify the stereoconfigurations with acyclic monomers being investigated for comparison.

RESULTS AND DISCUSSION

1. Photo-RAFT SUMI mechanism and monomer selection for discrete oligomer synthesis

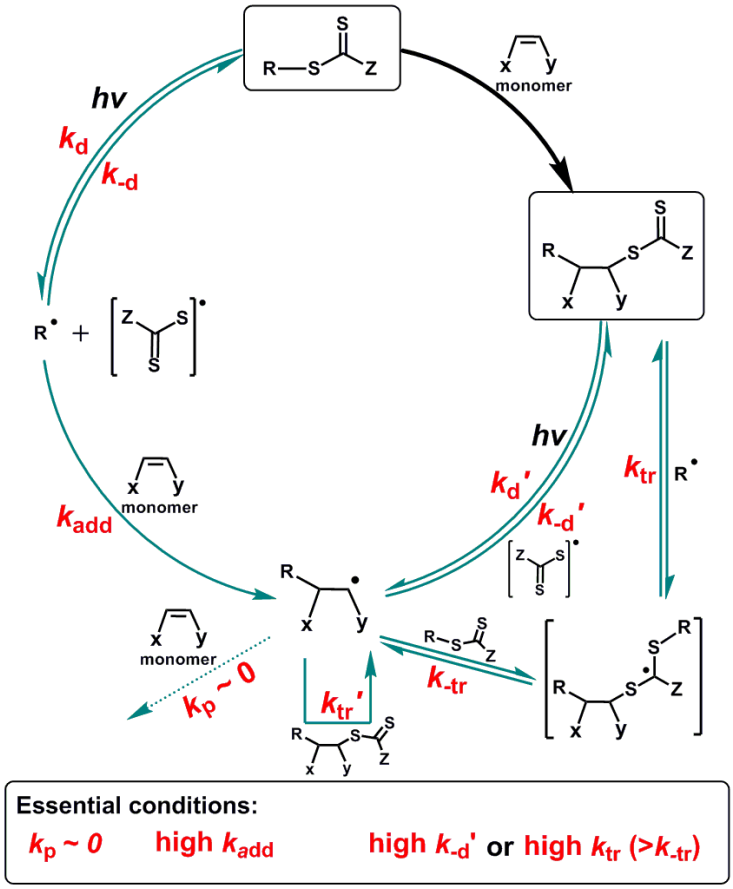

Scheme 1. Mechanism for photo-RAFT SUMI process and essential conditions for effective SUMI. k_d: decomposition rate constant of initial RAFT agent under light; k_{-d}: recombination rate constant of initial RAFT agent; k_{add}: addition rate constant of monomer to radical; k_p: propagation rate constant of monomer to its SUMI adduct radical; k_{tr}: chain transfer rate constant of SUMI adduct radical to initial RAFT agent; k_{-tr}: chain transfer rate constant of R group radical (R·) from initial RAFT agent to SUMI adduct macro-RAFT agent; k_{tr}': chain transfer rate constant of SUMI adduct radical to SUMI adduct macro-RAFT agent; k_d': decomposition rate constant of SUMI adduct macro-RAFT agent under light; k_{-d}': recombination rate constant of SUMI adduct macro-RAFT agent. For clarity, the PET-RAFT technique, which involves electron transfer in the presence of a photoredox catalyst, was not depicted in the scheme.

The reaction mechanism for light activated RAFT SUMI is proposed in **Scheme 1**, and is a photochemical development of the pioneering work of Zard and coworkers.[44] The initial RAFT agent (ZCS_2R) is activated under light to generate an R group radical (R·) and thiocarbonylthio anion or radical (ZCS_2·); this process can occur in the presence or absence of photocatalyst, depending on the employed RAFT agents and the irradiation wavelength. The R· radical can react with monomer to form a single monomer adduct radical, with the generation of the desired mono-adduct occurring through coupling with thiocarbonylthio anion or radical species, or alternatively, through an addition/fragmentation chain transfer process with dormant RAFT species. The latter pathway is accompanied by the generation of another R· radical through fragmentation of the RAFT radical intermediate species.

From the standpoint of the proposed mechanism, the monomer and RAFT agent selection plays a critical role in determining the success of SUMI. The ideal monomers for achieving single unit monomer addition are those which cannot radically homopolymerize (propagation rate constant, $k_p \sim 0$) but are able to alternatingly copolymerize with other monomers under a range of conditions, and with high monomer addition rate constants (k_{add}). Therefore, *α,β*-disubstituted and conjugated vinyl monomers, such as *N*-substituted maleimide (**Scheme 2a**) and Ind (**Scheme 2b**), are ideal candidates due to their superior capability for alternating copolymerization with high reaction rates. Moreover, most maleimide and Ind monomers have also been reported to be radically non-homopolymerizable, which limits the formation of homopolymer side products.[81] In addition, maleimide monomers are electron accepting, while Ind monomers are electron donating, leading to formation of a charge transfer complex and allowing for alternating copolymerization to occur with high reaction rates.[82] Maleic anhydride (MAn, **Scheme 2a**) presents similar reaction behavior as maleimide, however, there is a high potential for hydrolysis and thus ring opening during the reaction. Meanwhile, although maleate, fumarate and trans-*β*-methylstyrene (*Trans*-MeSt, **Scheme 2b**) have low k_p (~ 0),[81] their reaction yield for SUMI into RAFT agents are very low (SI**,** see Section 2.3), suggesting addition rates of these monomers are not as high as maleimides and Ind, and thus they are not ideal monomers for the SUMI process used in this study.

Another critical component in RAFT mediated SUMI reaction protocols is the selection of the chain transfer agent. The high decomposition rate constant (k_d) of RAFT agent (ZCS_2R) was essential to ensure rapid generation of the initiating radical; the k_d value is directly related to the C-S bond dissociation energy of RAFT agent. Employing the PET-RAFT (photoinduced electron/energy transfer - RAFT) technique[83-84] and a great variety of photoredox catalysts, most RAFT agents can be activated under light with high k_d. For instance, trithiocarbonate can be easily activated to generate radicals with high efficiency in the presence of zinc tetraphenylporphyrin (ZnTPP) under low energy red light.[85] Direct evidence of high k_d and k_{add} is the rapid consumption of RAFT agents (ZCS_2R) observed in these SUMI reactions.

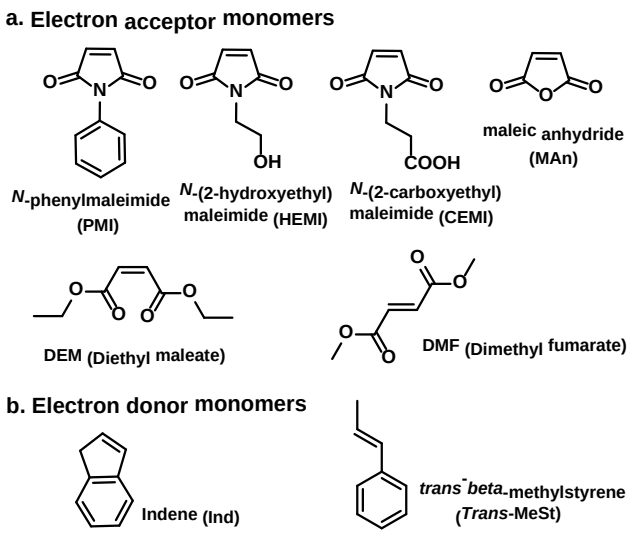

Scheme 2. Various *α,β*-di-substituted vinyl monomers (electron acceptor (a) and electron donor monomers (b)) investigated in this study.

The reaction of the carbon centered R group radical from the starting RAFT agent with the disubstituted monomers can also be manipulated through RAFT agent selection. For instance, *n*-butyl benzyl trithiocarbonate (BBTC, **Scheme 3**) with an electron donating benzyl group (R group) can react with electron acceptor monomers such as malemides, maleates and fumarates, but not electron donor monomers such as Ind and *Trans*-MeSt. The trithiocarbonate (CDTPC, **Scheme 3**) with an electron accepting cyano-isopropyl group (R group) reacts in the reverse way. Meanwhile, high monomer/RAFT ratios (> 1/1) may be necessary in specific cases to increase the rate of insertion. The excess monomer does not lead to the formation of undesired higher oligomers (dimers, trimers, etc.) through multiple insertions as the monomer will not homopolymerize (*vide supra*).

The other essential condition for effective SUMI processes is a high recombination rate constant (k_{-d}', k_{-d}'[ZCS_2·] >> k_p[Monomer] ~ 0), or high chain transfer rate constant ($k_{tr} > k_{-tr}$, k_{tr}[ZCS_2R] >> k_p[Monomer] ~ 0); this will ensure the effective formation of the SUMI adduct and prevent radical accumulation and undesirable termination reactions. Other factors such as a low decomposition rate constant (k_d') for the SUMI adduct are beneficial for the reaction efficiency and product purity but are not essential. Although it is difficult to determine the rate constants for these SUMI processes experimentally, qualitative estimates are helpful for understanding and optimizing such reactions.

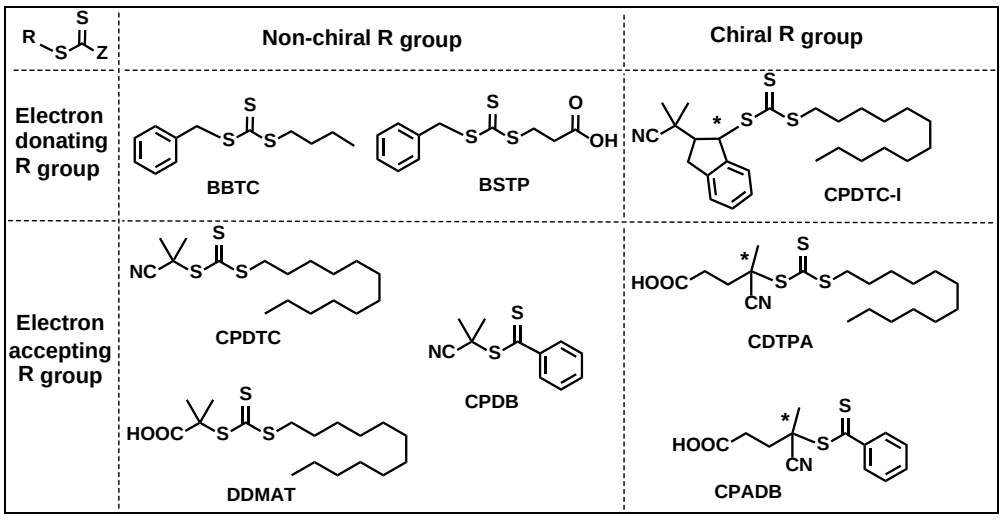

Scheme 3. Various RAFT agents with diverse R (leaving) groups investigated in this study. BBTC: *n*-butyl benzyl trithiocarbonate; BSTP: 3-benzylsulfanylthiocarbonylsulfanyl propionic acid; CPDTC: 2-cyano-2-propyl dodecyl trithiocarbonate; DDMAT: 2-(dodecylthiocarbonothioylthio)-2-methylpropionic acid; CPDB: 2-cyano-2-propyl dithiobenzoate; CPDTC-I: SUMI mono-adduct of indene inserted into CPDTC; CDTPA: 4-cyano-4-(((dodecylthio) carbonothioyl)thio)pentanoic acid; CPADB: 4-cyanopentanoic acid dithiobenzoate. The asterisk (*) indicates the chiral carbon.

2. Sequence control of discrete oligomers using sequential and alternating SUMI

The initial RAFT agent for the synthesis of discrete oligomers was screened from the selection shown in **Scheme 3**. Dithiobenzoates, CPDB and CPADB, are poor choices for sequential SUMI processes as their mono-adducts cannot be reactivated ($k_d \sim 0$) by common photocatalysts used for PET-RAFT technique.[46] All trithiocarbonates are suitable for SUMI reactions, but BBTC was selected as a model RAFT agent because it has the simplest chemical structure (benzyl R group and *n*-butylthiol Z group), which simplifies NMR analysis compared to other RAFT agents. For example, the chiral R group in CDTPA leads to doubled diastereomers in the final product and complicates NMR analysis. BBTC was synthesized using an analogous procedure to BSTP, which has been reported in previous literature.[83, 86] Following silica column purification, nearly 60 g of BBTC RAFT agent was obtained; with the lower polarity of BBTC compared to BSTP reducing the difficulty of the column purification process. Furthermore, while other trithiocarbonates (CPDTC, CDTPA and DDMAT, **Scheme 3**) are commercially available, they are still relatively expensive.

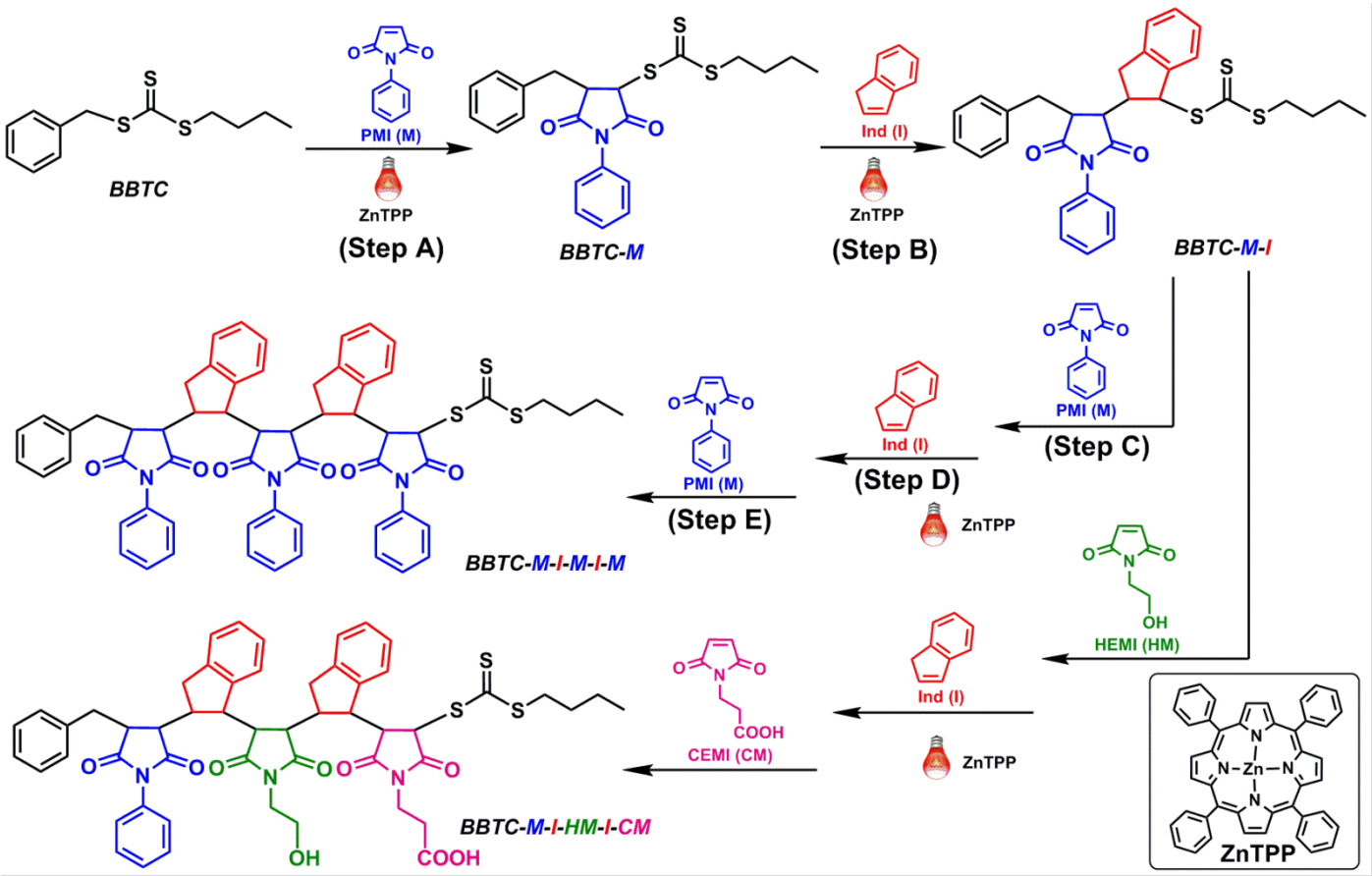

Scheme 4. Synthetic chemistry of two model discrete pentamers, BBTC-M-I-M-I-M and BBTC-M-I-HM-I-CM.

Two model pentamers, BBTC-PMI-Ind-PMI-Ind-PMI (denoted as BBTC-M-I-M-I-M) with alternating *N*-phenylmaleimide (PMI) and Ind, and BBTC-PMI-Ind-HEMI-Ind-CEMI (denoted as BBTC-M-I-HM-I-CM) (**Scheme 4**) with diverse functionalities, were synthesized to evaluate the reaction conditions and kinetic efficiency. There are two key SUMI steps which are repeated during the synthesis of

long oligomers: (1) the insertion of Ind to BBTC-M to generate BBTC-M-I, and (2) the insertion of maleimide into BBTC-M-I to generate BBTC-M-I-M. The reaction kinetics of both steps were comprehensively investigated using online monitoring techniques. The SUMI adducts were fully characterized by NMR, GPC and ESI-MS. The structural verification of long oligomers (> 5 monomer units) is challenging through NMR due to substantial signal overlap; as such, only GPC and ESI-MS were used for characterization of the pentamers.

2.1 Synthesis of BBTC-M mono-adduct in Step A

We started the SUMI process by activating BBTC through the PET-RAFT technique in the presence of PMI. Following the design principles outlined in Section 1, a suitable electron donor-acceptor pair between the donating BBTC R group (benzyl) and maleimide acceptor was formed, leading to effective SUMI of PMI into BBTC. The reaction was performed in the presence of ZnTPP as photocatalyst under red light, using the molar ratio of [PMI]:[BBTC]:[ZnTPP] =1/1/0.005. The kinetic profile of this reaction was determined by monitoring the conversion of BBTC against time using online ^{1}H NMR spectroscopy using deuterated DMSO as reaction solvent (**Figure 2a**). The reaction proceeded quickly within the first 2 h and slowed down to reach 65% after 10 h of irradiation. With the consumption of BBTC, the concentration of BBTC-M increased and reached an equilibrium stage. The conversion of RAFT agent could not reach 100% since the benzyl radical in BBTC is a poorer leaving group than the maleimidyl radical of the newly formed SUMI adduct (BBTC-M). The light activation and addition/fragmentation process of BBTC-M competes with that of BBTC, i.e., k_d[BBTC] competes with $k_{d'}$[BBTC-M], while k_{tr}[BBTC] competes with k_{-tr}[BBTC-M]. The decomposition rate of BBTC-M is higher than that of BBTC (k_d' > k_d) due to the lower C-S bond dissociation energy of BBTC-M compared with BBTC. The chain transfer rate k_{-tr} is higher than k_{tr} in this SUMI, which suggests fragmentation to produce SUMI product of BBTC-M (SI, **Scheme S1**) is unfavorable.

The stacked ^{1}H NMR spectra (SI, **Figure S3**) at different time points (0, 1, and 9 h) clearly showed the SUMI process proceeded smoothly without obvious side reactions, such as RAFT agent degradation by irreversible termination and dimer formation (BBTC-M-M). The crude mono-adduct was purified by column chromatography to give an isolated yield of 56%. Although a higher [PMI]/[BBTC] ratio such as 5/1 could potentially increase the yield, it is not atom-economic and will increase the risk of multiple monomer insertion. Neat ^{1}H and ^{13}C NMR spectra (SI, **Figure S4** and **S5**) clearly confirmed the chemical structure and high purity of the mono-adduct. ESI-MS (**Figure 3c** and SI, **Figure S6**) further confirmed the isolated product is BBTC-M.

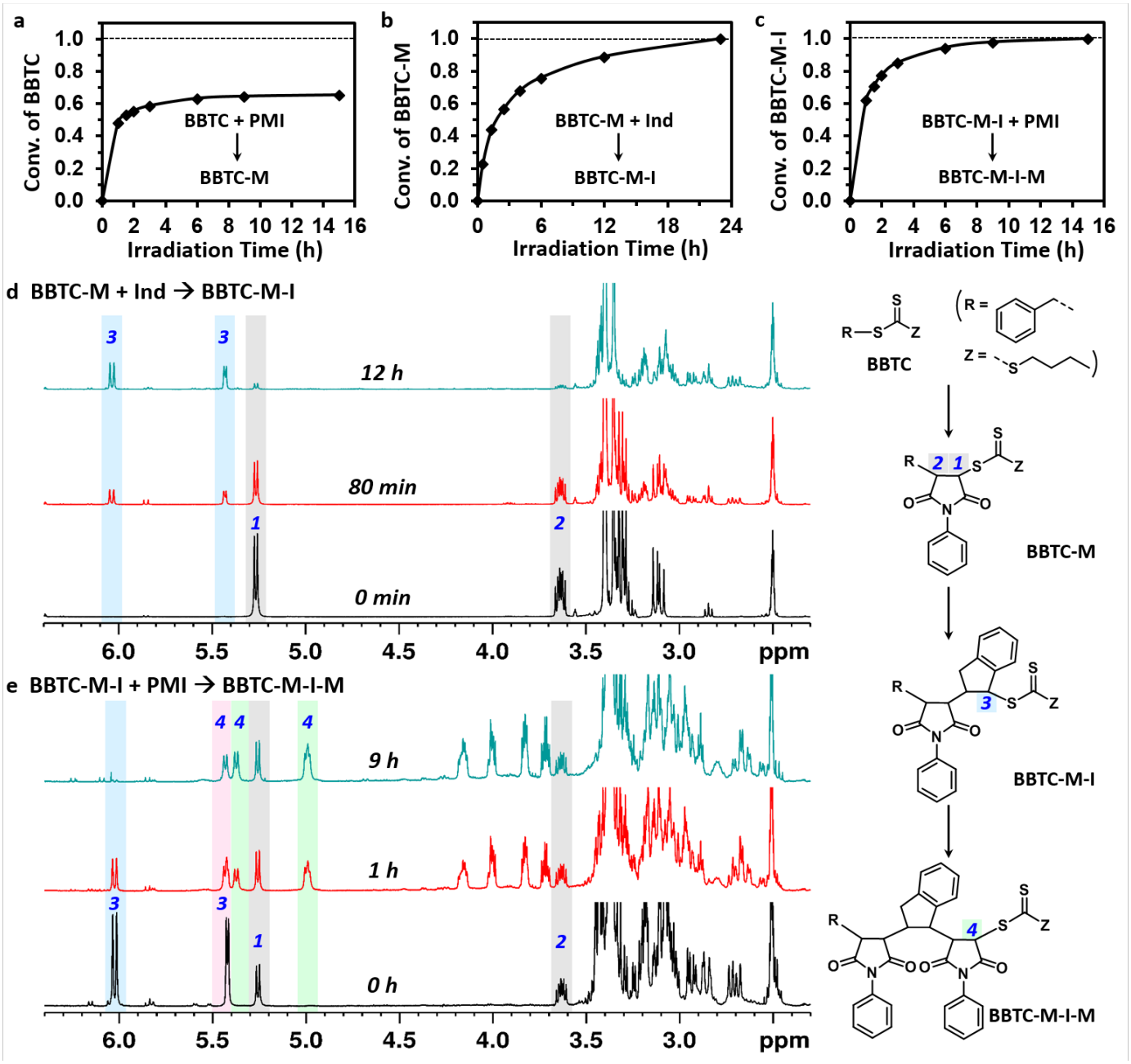

Figure 2. Kinetic study of sequential PET-RAFT SUMI processes from BBTC to BBTC-M-I-M monitored by online ^{1}H NMR analysis (DMSO-d_6, 400 MHz). Conversions of RAFT agents *versus* irradiation time: BBTC (**a**), BBTC-M (**b**) and BBTC-M-I (**c**); Stacked ^{1}H NMR spectra indicated the SUMI processes: BBTC-M to BBTC-M-I (**d**) and BBTC-M-I to BBTC-M-I-M (**e**). The scheme on the right depicts the corresponding chemical structures of the growing SUMI products examined in this kinetic study.

2.2 Synthesis of BBTC-M-I dimer in Step B

The insertion of Ind to BBTC-M to prepare BBTC-M-I followed a similar process to Step A, with identical reaction conditions employed, except for a higher monomer/RAFT ratio ([Ind]:[BBTC-M]:[ZnTPP] = 5/1/0.005). An increased monomer/RAFT ratio was used due to the relatively low addition rate of Ind to maleimidyl radicals, compared to that of PMI to benzyl radicals. In this step, the proposed reaction pathway is similar with Step A (k_d' > k_d and k_{-tr} > k_{tr}), as shown in the SI, **Scheme S2**. The slightly higher stability of

Ind radicals compared to maleimidyl radicals causes $k_d' > k_d$, and also leads to the favorable fragmentation of intermediate to generate the Ind radical not the SUMI product (BBTC-M-I). Therefore, the high monomer/RAFT ratio improves the RAFT agent conversion and reaction yield by pushing the reaction towards the desired SUMI product (BBTC-M-I), although it also increases the probability of dimer formation.

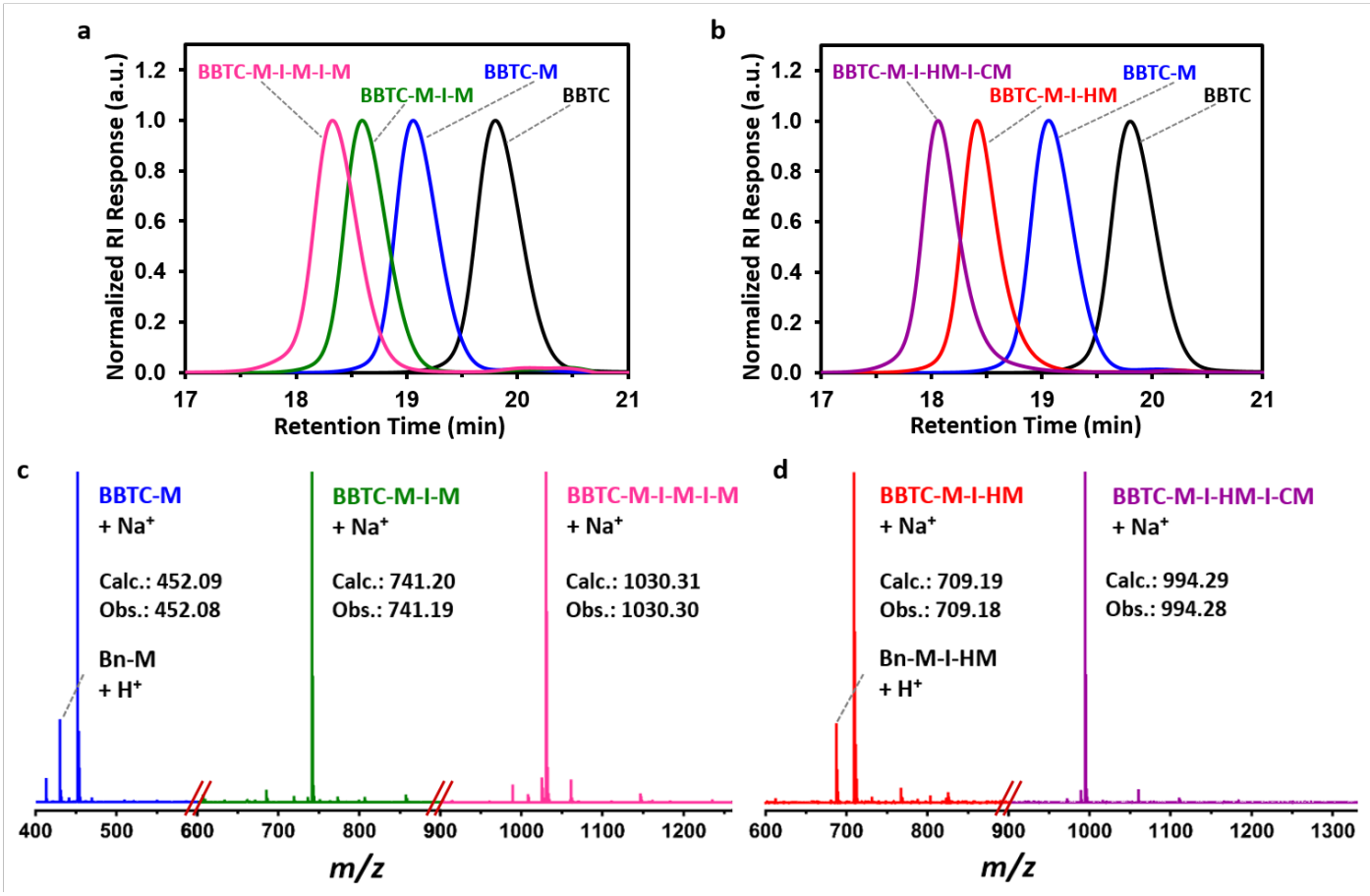

Figure 3. GPC traces and ESI-MS spectra for all SUMI adducts. GPC traces for the successive synthesized oligomers, from BBTC to BBTC-M-I-M-I-M (a) and from BBTC to BBTC-M-I-HM-I-CM (b), and their corresponding ESI-MS spectra (c) and (d). The full spectra for these SUMI adducts can be found in Supporting Information.

The reaction kinetics showed the conversion of macro-RAFT agent, BBTC-M, reached 100% after 20 h of irradiation (**Figure 2b**). ^{1}H NMR showed the reaction proceeded smoothly with the increased doublet peak signals at δ 5.42 ppm and δ 6.05 ppm assigned to the two diastereomers of the terminal –CH– proton (proton *3*) in BBTC-M-I (**Figure 2d**). The peak signals at δ 5.28 ppm and δ 3.65 ppm assigned to the protons *1* and *2* dropped to 10 % as the reaction time increased from 0 h to 12 h. After 20 h of irradiation, a signal peak (*m/z* = 684.20) in ESI-MS was observed, which suggested the presence of double Ind insertion (BBTC-M-I-I) ionized with Na^+ (SI, **Figure S7b**). The double insertion is attributed to the low chain transfer rate ($k_{-tr} > k_{tr}$), causing an increased probability of multiple monomer insertion after long irradiation times in

the presence of excess monomer. Fortunately, a shorter reaction time (< 15 h) effectively suppressed the formation of this Ind double insertion adduct (ESI-MS, SI, **Figure S7a**). As a result, the RAFT conversion in Step B had to be limited to 85~95%. However, it is not necessary to push macro-RAFT conversion to 100%; the unreacted BBTC-M will be unable to participate in the subsequent maleimide insertion reaction in Step C, as the low maleimide homopolymerization rate ($k_p \sim 0$) suppresses the formation of the dimeric BBTC-M-M adduct. More importantly, this unreacted BBTC-M can be easily removed by column chromatography to afford pure BBTC-M-I-M trimer in Step C (*vide infra*). The ^{1}H NMR spectrum for the crude product after excess monomer (Ind) removal clearly demonstrated the presence of a mixture of BBTC-M-I and BBTC-M (SI, **Figure S8**).

2.3 Synthesis of BBTC-M-I-M trimer in Step C

This step involves the highly efficient insertion of PMI into BBTC-M-I dimer to form the BBTC-M-I-M trimer, which differentiates the insertion of PMI into BBTC in Step A due to a different R group (benzyl radical *versus* Ind radical). Ind radicals are better leaving groups than both benzyl and maleimidyl radicals, and thus the insertion of PMI into BBTC-M-I reached high conversions (95% isolated yield). The high chain transfer rate ($k_{-tr} < k_{tr}$) made the intermediate species preferentially generate the trimer SUMI adduct rather than the RAFT dimer and trimer adduct radical (SI, **Scheme S3**). The high decomposition rate ($k_d' < k_d$) also allowed for fast conversion of the RAFT agent (BBTC-M-I), which was reflected in the kinetic results (**Figure 2c**). Nearly full conversion of the initial RAFT agent (BBTC-M-I) was observed after 15 h of irradiation, with a molar ratio of [PMI]/[BBTC-M-I] = 1/1. The ^{1}H NMR spectra (**Figure 2e**) at different time points of the reaction (0, 1, and 9 h) clearly indicated the gradual consumption of BBTC-M-I dimer by the decrease of the peak signals at δ 5.42 and δ 6.05 ppm assigned to the proton *3* of terminal –CH- in the dimer BBTC-M-I, and generation of BBTC-M-I-M trimer by the increase of peak signals at δ 5.44, δ 5.38 and δ 5.0 ppm, assigned to the proton *4* of terminal –CH– in the trimer BBTC-M-I-M. As anticipated, the unreacted BBTC-M mono-adduct (the peak signals for protons *1* and *2* in BBTC-M at 0 h) remained intact during the reaction, which demonstrates that the presence of this species (from the previous insertion step) does not affect the production of the target trimer. The unreacted BBTC-M can simply be removed by conventional column chromatography. The R_f values in silica gel thin layer chromatography (TLC) for the impurity, BBTC-M, and the product, BBTC-M-I-M, are very different (R_f = 0.7 for BBTC-M and 0.3 for BBTC-M-I-M using 5/1 (v/v) hexane/ethyl acetate as the eluent), due to the increased polarity and molecular mass of BBTC-M-I-M. The ^{1}H NMR spectra also indicated that other side reactions (multiple maleimide insertion or RAFT agent degradation) were negligible.

After purification by column chromatography, the structure of the isolated BBTC-M-I-M trimer was

verified by ^{1}H and ^{13}C NMR, HSQC, and HMBC (SI, **Figure S9, S10, S11 and S12**). The ^{1}H NMR spectrum is complicated due to the presence of several diastereomers for this compound. Furthermore, the ^{1}H NMR spectrum measured in $CDCl_3$ (SI, **Figure S9**) was different to that in DMSO-d_6 (**Figure 2e**). Particularly, the terminal –CH– proton shows different chemical shifts and profiles, which gives three peaks from δ 4.9~5.5 ppm in DMSO-d_6 and two peaks from δ 4.6~4.9 ppm in $CDCl_3$. Moreover, the peaks from δ 4.6~4.9 ppm in $CDCl_3$ are not all signals of terminal –CH– proton in these molecules, which was demonstrated by the low integration values of the peaks. The other part of the signal for this proton is overlapped in the area from δ 3.95~4.15 ppm, which was demonstrated by the analysis of ^{13}C NMR (SI, **Figure S10**), high resolution ^{1}H-^{13}C HSQC (SI, **Figure S11**), and ^{1}H-^{13}C HMBC (SI, **Figure S12**). HSQC confirmed the rough assignment of every proton in the molecule and HMBC confirmed the peak location of the terminal –CH– proton. To further confirm the structure of the synthetic compound, GPC and ESI-MS analysis was performed. The GPC trace for this product showed a unimodal and symmetric peak, and a clear shift in molecular weight compared to BBTC-M (**Figure 3a**). ESI-MS confirmed the molar mass of the product to be 741.19, which matched well with the target compound ionized with Na^+ (**Figure 3c and SI, Figure S13**). A more detailed discussion for the structural verification of this compound can be found in Supporting Information.

2.4 Synthesis of BBTC-M-I-M-I tetramer in Step D and BBTC-M-I-M-I-M pentamer in Step E

The tetramer and pentamer were successfully synthesized and isolated using the same procedures as those for dimer and trimer synthesis under identical conditions in high yield (85% isolated yields for two reaction steps). A conventional silica column was employed to remove excess monomer and trace amounts of impurities, however, difficulties in purification arose due to reduced discrepancy in both molecular weights and polarity between two neighboring SUMI products. The final purified products were confirmed by ^{1}H NMR (SI, **Figure S14** for BBTC-M-I-M-I tetramer and **Figure S16** for BBTC-M-I-M-I-M pentamer), GPC (**Figure 3a**) and ESI-MS (**Figure 3c** and SI, **Figure S15** for BBTC-M-I-M-I tetramer and **Figure S17** for BBTC-M-I-M-I-M pentamer).

According to the reaction conditions and efficiency, the trithiocarbonate end group in each step can always be activated easily in the co-monomer system. The SUMI process described in this work can therefore be repeated numerous times with the biggest challenge being separation of the product adducts from the reaction mixture. However, the use of a support resin similar to those used in solid-phase peptide synthesis could potentially increase the commercial viability of this SUMI process.

To demonstrate the end-group fidelity and the capability of the pentamer as a functional building block

for constructing complex polymer architectures, the synthesized BBTC-M-I-M-I-M pentamer was employed as macro-RAFT agent for the polymerization of methyl acrylate (MA) to prepare diblock copolymer ((BBTC-M-I-M-I-M)-*b*-poly(MA)) using the PET-RAFT technique with ZnTPP as the photocatalyst. The kinetic plots of M_n *versus* monomer conversion, $\ln([M]_0/[M]_t)$ *versus* exposure time and molecular weight distribution were investigated. The linear increase of $M_{n,GPC}$ *versus* monomer conversion (**Figure 4b**) demonstrated that this macro-RAFT agent was able to mediate the controlled radical polymerization of MA. The experimental molecular weights at different monomer conversions were slightly higher than the theoretical values calibrated by polystyrene standards, which was attributed to the molecular weight of macro-RAFT agents. Regardless, the uniform and symmetric molecular weight distributions showed no signs of tailing and the clear and complete shift in molecular weight indicated the remarkable living character and end-group fidelity of macro-RAFT agents (**Figure 4d**). Moreover, the dispersity (M_w/M_n in **Figure 4b**) was as low as 1.08 during polymerization, illustrating that the pentamer is an excellent chain transfer agent. Additionally, "ON"/"OFF" experiments revealed that the polymerization process can be started and stopped by switching the light "ON" and "OFF" (**Figure 4a**); similar temporal control has been demonstrated previously in other PET-RAFT polymerization systems.[46, 85, 87]

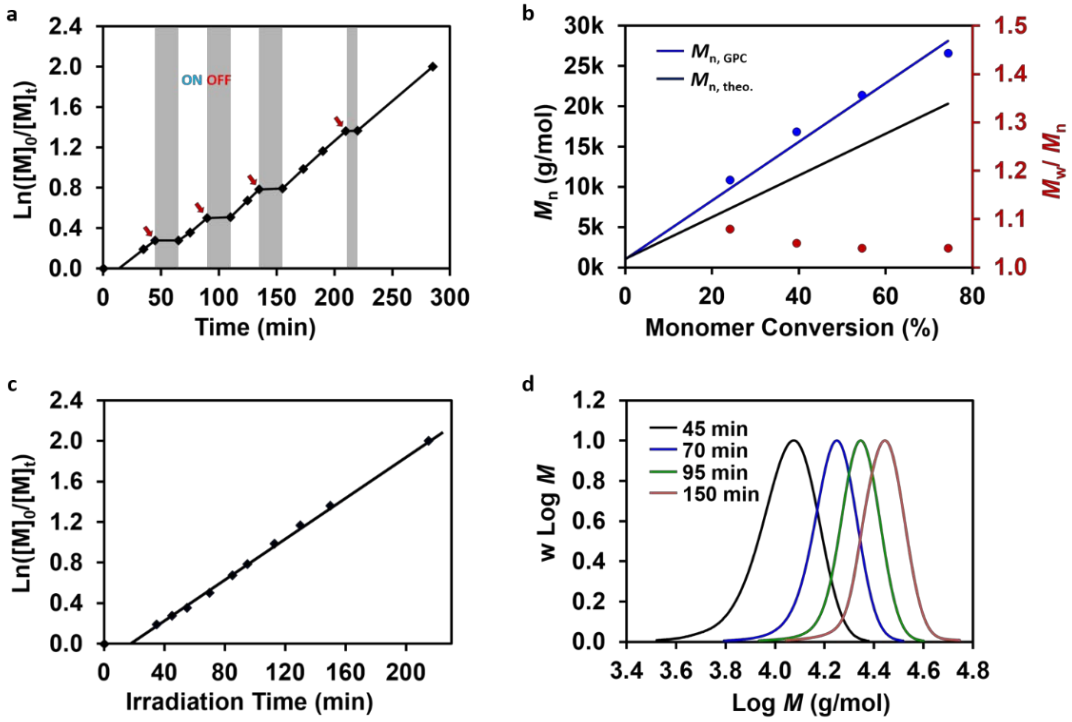

Figure 4. Online Fourier transform near-infrared (FTNIR) measurement for kinetic study of PET-RAFT polymerization of methyl acrylate (MA), using pentamer BBTC-M-I-M-I-M as macro-RAFT agent and ZnTPP as photocatalyst, with the molar ratio of [MA]:[macro-RAFT]:[ZnTPP] = 300:1:0.01 (~33 ppm catalyst with respect to monomer concentration): **(a)** monomer conversion *versus* time in the presence (ON) or in the absence (OFF) of light, red arrows represent the four sampling time points for GPC analysis; **(b)** M_n and M_w/M_n *versus* conversion; **(c)** $\ln([M]_0/[M]_t)$ *versus* irradiation time and **(d)** molecular weight

distributions at different time points.

2.5 BBTC-M-I-HM trimer and BBTC-M-I-HM-I-CM pentamer

A range of other functional trimers and pentamers were prepared by simply following the same synthetic protocol as those for BBTC-M-I-M trimer and BBTC-M-I-M-I-M pentamer, except that the maleimide monomers were changed to HEMI and CEMI (**Scheme 2**) for the third and fifth monomer insertion instead of PMI (**Scheme 4**). The purification procedures were also similar, using conventional silica gel column and gradient solvents, except that the composition of solvents was a little different due to increased polarity of the new SUMI compounds. The product for each step was fully characterized by ^{1}H NMR (SI, **Figure S18, S20** and **S21**) with GPC (**Figure 3b**) and ESI-MS (**Figure 3d** and SI, **Figure S19 and S22**) of the trimer and pentamer providing solid evidence of successful production in high purity. Significantly, the isolated yields were 95% and 86% for the trimer and pentamer, respectively.

3. Stereospecificity of synthetic discrete oligomers

The properties of natural and synthetic polymers are determined in large part by geometrical and stereogenic structures, i.e., degree of regularity of the chemical substituents along macromolecular chain. In general, high regularity imparts strength, high glass transition temperatures and hardness, together with restricted solubility in solvents. Symmetry and regularity in macromolecular structures also enhances micro-crystallinity, which is a key property for many applications of polymeric materials. Designing and tuning micro-crystallinity of polymers at the molecular level is therefore a fundamental challenge for synthetic chemists.

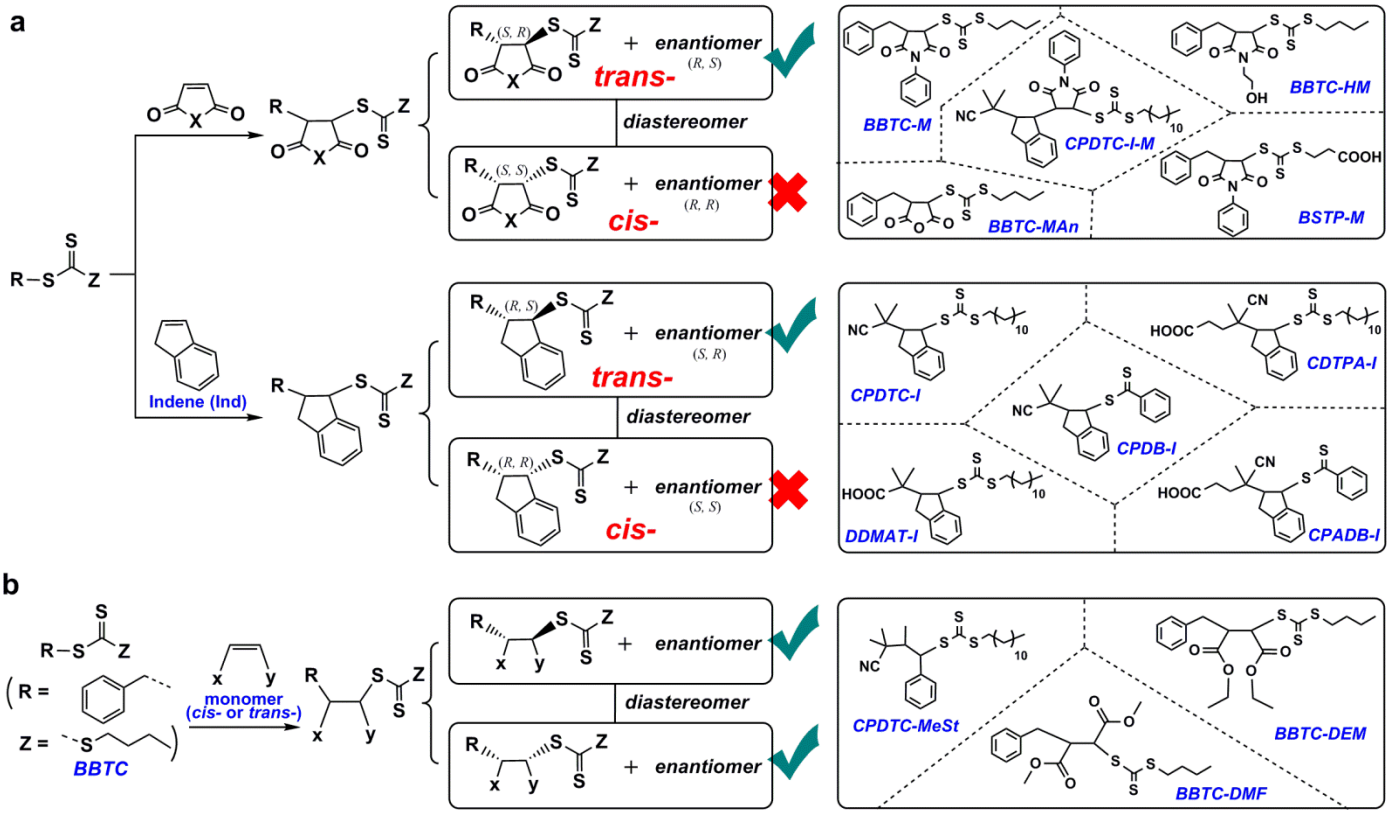

Scheme 5. (a) Photo-RAFT SUMI of cyclic monomers into various RAFT agents generating single monomer adducts with all-*trans* configuration; (b) Photo-RAFT SUMI of acyclic monomers to RAFT agent (BBTC) generating SUMI adducts with mixed *cis*- and *trans*- configurations.

Having demonstrated the ability to control the sequence and chain length of synthetic oligomers, our attention was turned to stereochemistry. As discussed previously in the characterization of synthetic oligomers (Section 2), full structural determination of compounds with more than three monomer units is difficult by NMR spectroscopy. Conveniently, it is not necessary to determine the stereoconfiguration for the full length of final oligomer, as the oligomer is composed of repeating alternative monomer units of *N*-substituted maleimide and Ind; if we can determine the stereoregularity of one repeating unit, it will be the same for all repeating units with increasing chain length. Initially, the stereochemistry of maleimide and

Ind independently inserted into various RAFT agents with chiral and non-chiral R groups was studied (**Scheme 5**). Maleic anhydride and three acyclic monomers, DEM, DMF and *Trans*-MeSt, were also investigated for comparison.

3.1 Stereochemistry of *N*-substituted maleimide unit in discrete oligomers

In the chain growth polymerization of asymmetric vinyl monomers, each propagation step results in the formation of either one (*α*-substituted and *α*,*α*-disubstituted monomers) or two (*α*,*β*-disubstituted) stereogenic centers with four different substituents for each. For *α*,*β*-disubstituted monomers, both backbone atoms are stereogenic with each possessing either *R* or *S* configuration. For the *α*,*β*-disubstituted cyclic vinyl monomers, four potential backbone configurations (*R*, *R*), (*R*, *S*), (*S*, *R*) and (*S*, *S*) exist; a pair of *cis*-enantiomers and a second pair of *trans*- enantiomers. With increasing degree of polymerization, the number of possible diastereomers rises exponentially and higher order stereochemical classification (e.g. *threo* and *erytheo*) becomes necessary.

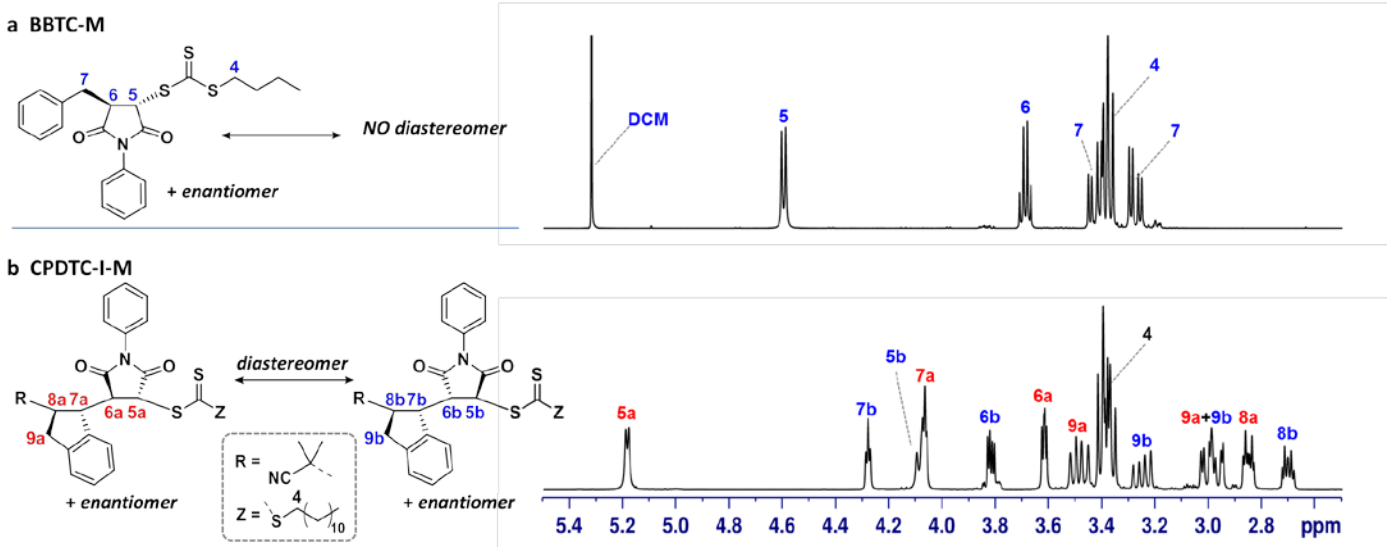

Figure 5. ^{1}H NMR spectra (400 MHz, $CDCl_3$) (δ 2.5~5.5 ppm) to demonstrate the *trans*- configuration of maleimide unit in purified (a) BBTC-M and (b) CPDTC-I-M.

During the SUMI of PMI into trithiocarbonate of BBTC, the fragment radicals can theoretically add to the maleimide double bond in both *cis*- and *trans*- fashions. Therefore, the mono-adduct of BBTC-M gives two diastereomers of *cis*- and *trans*- configurations in five-member ring units with their corresponding enantiomers of mirror-image molecules (**Figure 5a**). The *cis*- and *trans*- diastereomers have different stereogenic structures and molecular environments for the corresponding protons. Therefore, ^{1}H NMR analysis, particularly the chemical shifts and coupling constants (*J* values) of specific protons, can provide information to distinguish between *cis*- and *trans*- configurations. However, the ^{1}H NMR spectrum (**Figure 6a** and SI, **Figure S4**) of BBTC-M showed only one set of diastereotopic signals, implying formation of either a *cis*- or *trans*- configuration exclusively. The signal at δ 4.6 ppm was assigned to the proton of –CH–

(5) giving a doublet, which is coupled with the proton of –CH– (6) and showed the same coupling constant of $J_{H5,H6}$ = 7.2 Hz. The other configuration (either *cis*- or *trans*-) is supposed to show another doublet signal for the proton of –CH– (5), but was not observed.

The stereochemistry of *N*-substituted maleimides has interested researchers since 1960s in attempting to use homo- and co-polymerization to prepare polymers with helix-sense chirality.[88-89] The anionic homopolymerization of maleimides provided all-*trans* configuration at low (-78 °C) to room temperature with anionic initiators.[90] Radical homopolymerization of maleimides at elevated temperature (100 °C) with the assistance of chiral solvent or catalyst also showed *trans*- stereo-configuration.[91] The radical copolymerization of maleimides and styrene or propylene provided a helical structure, with the maleimide monomers most likely possessing an all *trans*- configuration.[88] In contrast, the electron-donor-acceptor interaction of styrene and cyclic citraconic anhydride (a maleic derivative) resulted in a mixture of *cis*- and *trans*- configurations.[92] Additionally, the single monomer radical addition of PMI to a xanthate gave a *trans*-configuration due to the steric hindrance.[44-45, 93] However, the chemical structure of the products was not comprehensively confirmed.

Due to the challenge of structural characterization of complex polymers, the stereochemical outcome of maleimide polymerization is thus arguable. There are no effective tools for polymers with large numbers of repeating monomer units, and as noted above previous experiments have delivered conflicting results. In contrast, SUMI provides an excellent tool to synthesize discrete oligomers with exact molecular weights, making it possible to confirm the stereoconfiguration and reaction mechanism, using widely used analytical equipment (NMR and XRD, etc). Most importantly, this tool can be applied to any monomers on the condition that they can be polymerized by iterative SUMI. In this study, the SUMI adducts of α,β-disubstituted vinyl monomers were synthesized and their stereochemistry was investigated for the first time. Particularly, this approach is able to assess the stereospecific configuration of our synthetic discrete oligomers in Section 2.

To elucidate the *cis*- or *trans*- configuration of the product of SUMI of PMI into trithiocarbonates, we performed single crystal X-ray diffraction (XRD) analysis and computational simulations. Single crystal XRD is a powerful technique that provides accurate structural information on small organic compounds, including the location of atoms, bond lengths, bond angles and stereo-configuration. The sample for XRD requires a crystalline compound, therefore, crystallization of mono-adduct compound, BSTP-M (**Scheme 5a**, ^{1}H NMR shown in SI, **Figure S23**) was carefully performed; BSTP-M was selected rather than BBTC-M due to the carboxylic acid moiety in BSTP, which facilitates more efficient crystallization. Fine needle-like crystals were obtained, suggesting that BSTP-M has good crystallinity and thus structural stereoregularity, as crystallinity is often regarded as external manifestation of a regular arrangement at the molecular level.

XRD analysis of the obtained crystal perfectly matched with the expected molecular structure of BSTP-M and unambiguously demonstrates that PMI insertion results in a *trans*- configuration (**Figure 6a**).

In agreement with the XRD results, computational modelling indicates that the *trans*-BSTP-M diastereomer is around 12.4 kJ/mol more stable than the corresponding *cis*-isomer (**Figure 6b**). This Gibbs-Free energy corresponds to a thermodynamic selectivity of over 99% for the *trans*- diastereomer (at room temperature), indicating that the PMI insertion into BSTP is highly stereospecific.

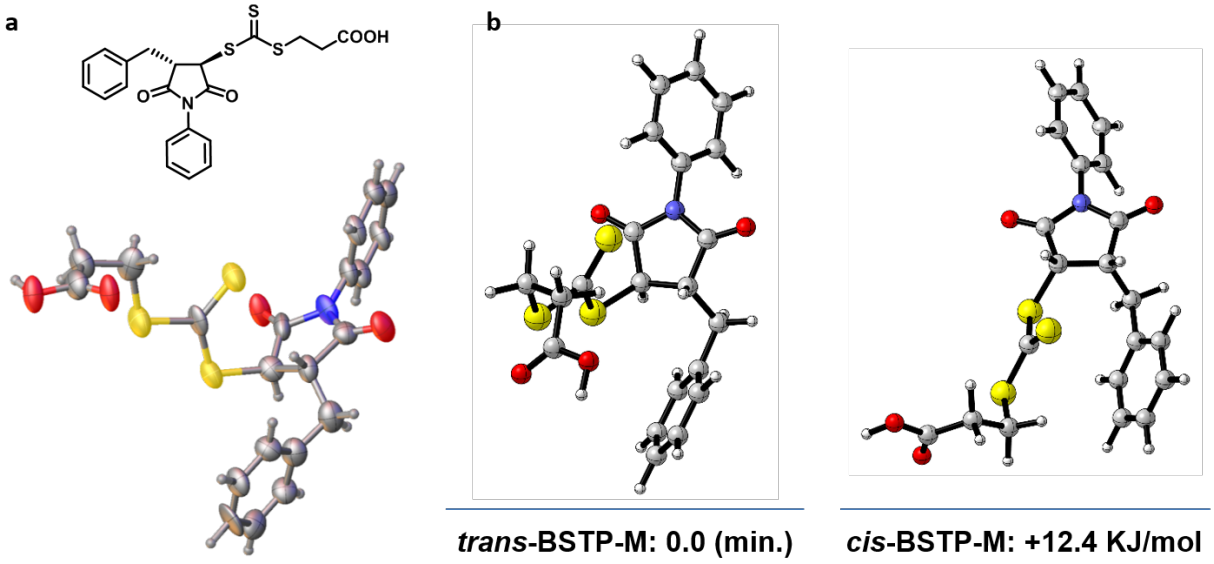

Figure 6. Single crystal XRD of BSTP-M (a) and modeling results showing the most stable conformations of the *trans*- and *cis*- BSTP-M diastereomers as well as their respective solution-phase Gibbs-Free Energies (b).

To illustrate the broad applicability of this strategy, *N*-substituted maleimide monomer, HM, and maleic anhydride (MAn) were also used to prepare the corresponding SUMI adducts BBTC-HM and BBTC-MAn (**Scheme 5a**). The ^{1}H NMR spectroscopy (SI, **Figure S28** and **S29**) revealed the same stereospecific preference for *trans*- configurations of HM and MAn units in the adducts, suggesting cyclic maleic monomers have the same stereogenic preference regardless of their substitution.

The RAFT agents of both BBTC and BSTP have non-chiral R groups. To investigate RAFT agents with chiral R groups, the insertion of PMI into CPDTC-I was performed and the resulting product analyzed by NMR (**Scheme 5a**). Careful analysis of the NMR results can be used to elucidate the stereochemical configuration of the PMI unit in the adduct (**Figure 5b** and SI, **Figure S32**). These NMR results indicate the same *trans*- configuration of the PMI unit in the adduct. There are two series (a and b) of proton signals which are assigned to the two diastereomers of CPDTC-I-M, each containing a pair of enantiomers as verified by 2D NMR analysis (SI, **Figure S33-S35**). If both *trans*- or *cis*- configurations for PMI exist, there should be four diastereomers which are attributed to each configuration (*trans*- or *cis*-) with two different

connection types for the Ind R group (*threo* and *erytheo*). Thus, if all four diastereomers are generated four series of proton signals would be anticipated. However, only two series signals were observed in the ^{1}H NMR spectrum, which are assigned to two diastereomers of the *trans*- configurations shown in **Figure 5b**.

It is worth noting that the two chemical shifts of the same protons in the adduct, such as –C*H*–S– (5), were were highly sensitive to the adduct stereochemistry. The chemical shift for one diastereoisomer is δ 6.1 ppm and δ 5.2 ppm for the other, which is attributed to the aromatic ring current effect (SI, **Scheme S4**). This proton has a very different chemical environment in each of the two *trans*- diastereomers; in one isomer (*threo*) it is deshielded by the phenyl ring of the adjacent Ind unit and thus leads to higher chemical shift.

3.2 Stereochemistry of Ind unit in discrete oligomers

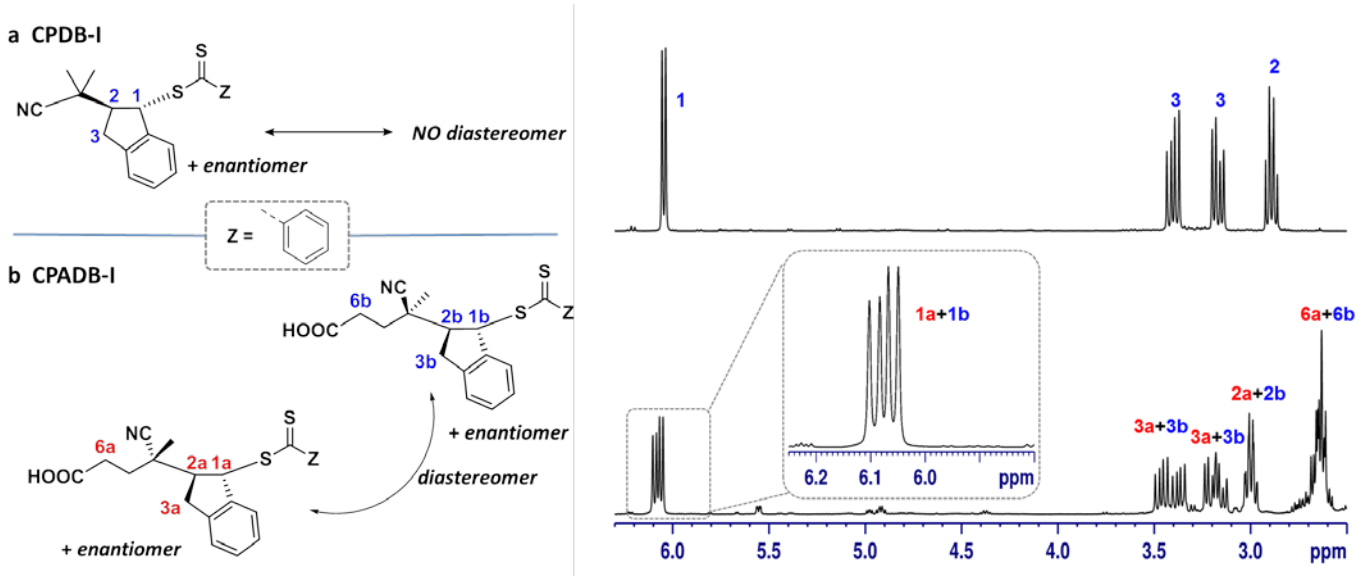

Figure 7. ^{1}H NMR spectra (400 MHz, $CDCl_3$) (δ 2.5~6.4 ppm) to demonstrate the *trans*- configuration of Ind in purified (a) CPDB-I and (b) CPADB-I.

As one of the alternating monomer units in these synthetic and discrete oligomers, Ind is different from maleimide due to its asymmetrical structure. Interestingly, there are no previous reports for its polymerization stereochemistry. Five RAFT agents with electron accepting R groups (**Scheme 3**) were therefore investigated for SUMI of Ind; three with non-chiral R groups and two with chiral R groups.

The characterization of these SUMI adducts was carried out by 1D and 2D NMR. For instance, the ^{1}H NMR of purified CPDB-I (**Figure 7a** and full spectrum shown in SI, **Figure S26**) was obtained to confirm the *trans*- configuration of the inserted cyclic Ind monomer with similar proton signals as that for BBTC-M being observed (**Figure 5a** and SI, **Figure S4**). Computational modelling also indicated that the *trans*-CPDB-I diastereomer is around 12.5 kJ/mol more stable than the corresponding *cis*-isomer (**Figure S27**). Other SUMI adducts including CPDTC-I (SI, **Figure S24**) and DDMAT-I (SI, **Figure S25**) had the same

stereospecific preference for *trans*- configurations as demonstrated by ^{1}H NMR results. In the case of chiral R group such as CPADB-I, the ^{1}H NMR spectrum (**Figure 7b** and full spectrum shown in SI, **Figure S30**) showed a more complicated signal pattern than the non-chiral R group of CPDB-I due to two diastereomers derived from the chiral carbon of the R group, in which two sets of signals were very closely positioned. For instance, the signal for proton 1 in **Figure 7b** (insert) at δ 6.02 ~ 6.15 ppm leads to two doublets centered at δ 6.06 ppm and 6.09 ppm, which belong to two different diastereomers. The CDTPA-I SUMI mono adduct had the same ^{1}H NMR profile (SI, **Figure S31**) as CPADB-I, attributed to the same chiral R group.

Computational modelling further confirmed the *trans*- configuration of Ind unit in the synthetic oligomers with the potential energy surface (PES) for the insertion of PMI into CPDTC-I being examined. In this reaction, the relative free-energy of four intermediate diastereomeric configurations (*threo-cis*, *erytheo-cis*, *threo-trans* and *erytheo-trans*, SI, **Figure S36**) was compared to determine the most favorable reaction pathways. The modelled conditions are identical to the experimental ones (solution-phase in DMSO, at 25 ^{o}C). The results clearly showed that both *trans*- insertion reactions are more kinetically favorable (> 10 kJ/mol) than either *cis*- insertion pathway, suggesting that the Ind unit also prefers *trans*-insertion as for the PMI unit.

3.3 Stereochemistry of acyclic monomer in discrete oligomers

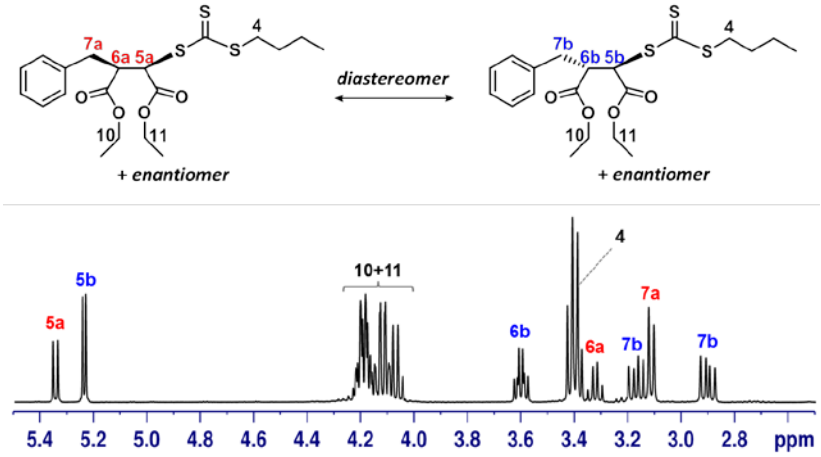

Figure 8. ^{1}H NMR spectra (400 MHz, $CDCl_3$) (δ 2.5~5.5 ppm) to demonstrate the *cis*- and *trans*- mixed configurations of DEM unit in purified BBTC-DEM.

As a comparison, the SUMI of acyclic monomers (**Scheme 2**) into RAFT agents did not show stereospecificity due to the lack of cyclic structure and a free rotating single bond along the backbone. For instance, the ^{1}H NMR spectrum of BBTC-DEM (**Figure 8** and SI, **Figure S39**) showed two series of proton signals (a and b) which belong to two diastereomers, each of them with a corresponding pair of enantiomers. The signals for the same protons in each diastereoisomer presented different chemical shifts (0.12 ppm

difference for the proton 5a and 5b of –C*H*–S–, 0.3 ppm for the proton 6a and 6b of –C*H*–CH–S–) and splitting patterns (doublet for the proton 7a and two quartets for proton 7b). 2D NMR (^{1}H-^{1}H COSY, ^{1}H-^{13}C HSQC and ^{1}H-^{13}C HMBC) was employed to confirm the structure and our conclusion. It is interesting to note that the integrals for two proton signals are different, which suggested that one of the diastereomers formed preferentially over the other during the SUMI process, presumably due to a difference in steric hindrance.

To summarize the above results, the stereospecificity in the SUMI process relies on the monomer structure; the cyclic monomer prefers *trans*- insertion regardless of the chirality of R groups, but the acyclic monomer shows a mixture corresponding to both *cis*- and *trans*- configurations. This can be attributed to steric hindrance and the restricted rotation of cyclic monomers during radical addition (or recombination step). In contrast, radical addition (or recombination) with acyclic monomers was not stereospecific due to free rotation around the single bond of the C-C backbone.

This stereochemical preference was independent of temperature and solvents. High temperature will not change the *trans*- opening of cyclic monomers (SI, **Figure S37).** Low polarity solvents, such as cyclohexane, was also shown to have no effect on the stereospecific insertion of cyclic monomer into RAFT agents (SI, **Figure S38)**. Similarly, the photocatalysts investigated in this work do not induce stereospecificity, because the *trans*- configuration is formed in both the presence and absence of photocatalysts. The synthetic conditions used to synthesize the SUMI adducts varied depending on the RAFT agents and monomers employed. For instance, BBTC-M and CPDTC-I were prepared through two distinct photocatalytic processes. The synthesis of BBTC-M, described in the first section employed the PET-RAFT technique to activate the RAFT agent BBTC to generate benzyl radical using a photocatalyst ZnTPP under red LED light, followed by PMI monomer addition to form the desired adduct. CPDTC-I was synthesized by direct photolysis of the RAFT agent CPDTC under blue LED light, and subsequent single Ind addition. This protocol is similar to that used for single styrene insertion into a trithiocarbonate, which was described in a previous report using the photo-RAFT SUMI approach.[49]

CONCLUSION

In this contribution, we report a robust and highly efficient method of sequential and alternating single unit monomer insertion for the preparation of discrete oligomers with sequence control and stereospecific configuration (*trans*-) of inserted cyclic monomers. Two families of cyclic monomers, indene and *N*-substituted maleimide, were inserted into RAFT agents alternatively one unit at a time in high reaction yields, which effectively controlled the monomer sequences. The structures were confirmed by an online

NMR kinetic study, GPC and ESI-MS. Moreover, for each investigated cyclic monomers, stereospecific *trans*-insertion was observed due to steric hindrance from the growing oligomer chain. The stereochemistry of these oligomer adducts was verified by 1D and 2D NMR and XRD and explained by quantum-chemical modelling. This methodology provides a versatile approach to synthesize discrete polymers with precise sequence and location of functionalities, while also illustrating a powerful synthetic pathway to model oligomers for the investigation of absolute structure (e.g. stereochemistry) of synthetic polymers.

ASSOCIATED CONTENT

Supporting information

Experimental details, NMR spectra and all raw computational data (Figures S1~S45, Tables S1, and Schemes S1~S5).This material is available free of charge via the Internet at http://pubs.acs.org.

Notes

The authors declare no competing financial interest.

AUTHOR INFORMATION

Corresponding authors

michelle.coote@anu.edu.au (M.C.)

cboyer@unsw.edu.au (C.B.)

j.xu@unsw.edu.au (J.X.)

ACKNOWLEDGEMENTS

J.X. acknowledges Australian Research Council (ARC) for the Future Fellowships (FT160100095). J.X., K.S. and M.K. acknowledge Venture Business Laboratory-Nagoya University for the financial support of visiting program. J.X. also acknowledges Dr. James Hook from Mark Wainwright Analytical Centre at the UNSW Sydney and Prof. Junpo He from Fudan University for valuable advice on NMR analysis. Single crystal X-ray data was acquired at Australian Synchrotron. The structure determination and refinement was carried out by Ms. Ena Luis in School of Chemistry at UNSW Sydney and Dr. Mohan Bhadbhade in Solid State and Elemental Analysis Unit, Mark Wainwright Analytical Centre at UNSW Sydney. M.L.C gratefully acknowledges a Georgina Sweet ARC Laureate Fellowship and generous allocations of supercomputing time on the National Facility of the Australian National Computational Infrastructure. C.J.H. thanks the

MRSEC program of the National Science Foundation (DMR-1720256).

REFERENCES

1. Lutz, J.-F.; Ouchi, M.; Liu, D. R.; Sawamoto, M., Sequence-Controlled Polymers. *Science* **2013,** *341* (6146).
2. Olatunji, O., Classification of Natural Polymers. In *Natural Polymers: Industry Techniques and Applications*, Olatunji, O., Ed. Springer International Publishing: Cham, 2016; pp 1-17.
3. Lutz, J.-F.; Lehn, J.-M.; Meijer, E. W.; Matyjaszewski, K., From precision polymers to complex materials and systems. *Nature Reviews Materials* **2016,** *1*, 16024.
4. Ouchi, M.; Terashima, T.; Sawamoto, M., Transition Metal-Catalyzed Living Radical Polymerization: Toward Perfection in Catalysis and Precision Polymer Synthesis. *Chemical Reviews* **2009,** *109* (11), 4963-5050.
5. Nakano, T.; Okamoto, Y., Synthetic Helical Polymers: Conformation and Function. *Chemical Reviews* **2001,** *101* (12), 4013-4038.
6. Lutz, J. F., Defining the Field of Sequence-Controlled Polymers. *Macromolecular Rapid Communications* **2017,** *38* (24), 1700582.
7. Okamoto, Y., Precision synthesis, structure and function of helical polymers. *Proceedings of the Japan Academy. Series B, Physical and Biological Sciences* **2015,** *91* (6), 246-261.
8. Merrifield, R. B., Solid phase peptide synthesis. I. The synthesis of a tetrapeptide. *Journal of the American Chemical Society* **1963,** *85* (14), 2149-2154.
9. Gait, M. J., *Oligonucleotide synthesis*. IRL press: 1984.
10. Martin, E., Quest for the chemical synthesis of proteins. *Journal of Peptide Science* **2016,** *22* (5), 246-251.
11. L., H.; G., B. H., Precision Polymers: Monodisperse, Monomer-Sequence-Defined Segments to Target Future Demands of Polymers in Medicine. *Advanced Materials* **2009,** *21* (32-33), 3425-3431.
12. Vandenbergh, J.; Reekmans, G.; Adriaensens, P.; Junkers, T., Synthesis of sequence-defined acrylate oligomers via photo-induced copper-mediated radical monomer insertions. *Chemical Science* **2015,** *6* (10), 5753-5761.
13. Cavallo, G.; Poyer, S.; Amalian, J. A.; Dufour, F.; Burel, A.; Carapito, C.; Charles, L.; Lutz, J. F., Cleavable Binary Dyads: Simplifying Data Extraction and Increasing Storage Density in Digital Polymers. *Angewandte Chemie* **2018,** *130* (21), 6374-6377.
14. Mutlu, H.; Lutz, J. F., Reading Polymers: Sequencing of Natural and Synthetic Macromolecules. *Angewandte Chemie International Edition* **2014,** *53* (48), 13010-13019.
15. Roy, R. K.; Meszynska, A.; Laure, C.; Charles, L.; Verchin, C.; Lutz, J.-F., Design and synthesis of digitally encoded polymers that can be decoded and erased. *Nature Communications* **2015,** *6*, 7237.
16. Lutz, J.-F., Coding Macromolecules: Inputting Information in Polymers Using Monomer-Based Alphabets.

Macromolecules **2015,** *48* (14), 4759-4767.

17. Hecht, S.; Fréchet, J. M. J., Dendritic Encapsulation of Function: Applying Nature's Site Isolation Principle from Biomimetics to Materials Science. *Angewandte Chemie International Edition* **2001,** *40* (1), 74-91.
18. Kramer, J. W.; Treitler, D. S.; Dunn, E. W.; Castro, P. M.; Roisnel, T.; Thomas, C. M.; Coates, G. W., Polymerization of Enantiopure Monomers Using Syndiospecific Catalysts: A New Approach To Sequence Control in Polymer Synthesis. *Journal of the American Chemical Society* **2009,** *131* (44), 16042-16044.
19. Porel, M.; Thornlow, D. N.; Phan, N. N.; Alabi, C. A., Sequence-defined bioactive macrocycles via an acid-catalysed cascade reaction. *Nat Chem* **2016,** *8* (6), 590-596.
20. Ouchi, M.; Badi, N.; Lutz, J.-F.; Sawamoto, M., Single-chain technology using discrete synthetic macromolecules. *Nat Chem* **2011,** *3* (12), 917-924.
21. Gormley, A. J.; Yeow, J.; Ng, G.; Conway, Ó.; Boyer, C.; Chapman, R., An Oxygen-Tolerant PET-RAFT Polymerization for Screening Structure–Activity Relationships. *Angewandte Chemie International Edition* **2018,** *57* (6), 1557-1562.
22. Yokozawa, T.; Yokoyama, A., Chain-Growth Condensation Polymerization for the Synthesis of Well-Defined Condensation Polymers and π-Conjugated Polymers. *Chemical Reviews* **2009,** *109* (11), 5595-5619.
23. Satoh, K.; Matsuda, M.; Nagai, K.; Kamigaito, M., AAB-Sequence Living Radical Chain Copolymerization of Naturally Occurring Limonene with Maleimide: An End-to-End Sequence-Regulated Copolymer. *Journal of the American Chemical Society* **2010,** *132* (29), 10003-10005.
24. Soejima, T.; Satoh, K.; Kamigaito, M., Main-Chain and Side-Chain Sequence-Regulated Vinyl Copolymers by Iterative Atom Transfer Radical Additions and 1:1 or 2:1 Alternating Radical Copolymerization. *Journal of the American Chemical Society* **2016,** *138* (3), 944-954.
25. Soejima, T.; Satoh, K.; Kamigaito, M., Monomer Sequence Regulation in Main and Side Chains of Vinyl Copolymers: Synthesis of Vinyl Oligomonomers via Sequential Atom Transfer Radical Addition and Their Alternating Radical Copolymerization. *ACS Macro Letters* **2015,** *4* (7), 745-749.
26. Gu, X.; Zhang, L.; Li, Y.; Zhang, W.; Zhu, J.; Zhang, Z.; Zhu, X., Facile synthesis of advanced gradient polymers with sequence control using furan-protected maleimide as a comonomer. *Polymer Chemistry* **2018,** *9* (13), 1571-1576.
27. Ji, Y.; Zhang, L.; Gu, X.; Zhang, W.; Zhou, N.; Zhang, Z.; Zhu, X., Sequence-Controlled Polymers with Furan-Protected Maleimide as a Latent Monomer. *Angewandte Chemie International Edition* **2017,** *56* (9), 2328-2333.
28. Ouchi, M.; Nakano, M.; Nakanishi, T.; Sawamoto, M., Alternating Sequence Control for Carboxylic Acid and Hydroxy Pendant Groups by Controlled Radical Cyclopolymerization of a Divinyl Monomer Carrying a Cleavable Spacer. *Angewandte Chemie International Edition* **2016,** *55* (47), 14584-14589.
29. Gody, G.; Zetterlund, P. B.; Perrier, S.; Harrisson, S., The limits of precision monomer placement in chain growth

polymerization. *Nature Communications* **2016,** *7*, 10514.

30. Wu, Z.; Liu, P.; Liu, Y.; Wei, W.; Zhang, X.; Wang, P.; Xu, Z.; Xiong, H., Regulating sequence distribution of polyethers via ab initio kinetics control in anionic copolymerization. *Polymer Chemistry* **2017,** *8* (37), 5673-5678.
31. Li, J.; He, J., Synthesis of Sequence-Regulated Polymers: Alternating Polyacetylene through Regioselective Anionic Polymerization of Butadiene Derivatives. *ACS Macro Letters* **2015,** *4* (4), 372-376.
32. Weiss, R. M.; Short, A. L.; Meyer, T. Y., Sequence-Controlled Copolymers Prepared via Entropy-Driven Ring-Opening Metathesis Polymerization. *ACS Macro Letters* **2015,** *4* (9), 1039-1043.
33. Gutekunst, W. R.; Hawker, C. J., A General Approach to Sequence-Controlled Polymers Using Macrocyclic Ring Opening Metathesis Polymerization. *Journal of the American Chemical Society* **2015,** *137* (25), 8038-8041.
34. Zeng, F. R.; Ma, J. M.; Sun, L. H.; Zeng, Z.; Jiang, H.; Li, Z. L., Optically Active Precision Aliphatic Polyesters via Cross-Metathesis Polymerization. *Macromolecular Chemistry and Physics* **2018,** *219* (10), 1800031.
35. Satoh, K.; Ozawa, S.; Mizutani, M.; Nagai, K.; Kamigaito, M., Sequence-regulated vinyl copolymers by metal-catalysed step-growth radical polymerization. *Nature Communications* **2010,** *1*, 6.
36. Tong, X.; Guo, B.-h.; Huang, Y., Toward the synthesis of sequence-controlled vinyl copolymers. *Chemical Communications* **2011,** *47* (5), 1455-1457.
37. Chun-Hao, W.; Zi-Yuan, S.; Xin-Xing, D.; Li-Jing, Z.; Fu-Sheng, D.; Zi-Chen, L., Combination of ATRA and ATRC for the Synthesis of Periodic Vinyl Copolymers. *Macromolecular Rapid Communications* **2014,** *35* (4), 474-478.
38. Sandra, B.; Denis, D.; A., C. L.; J., H. C.; Eric, D., Precise Synthesis of Molecularly Defined Oligomers and Polymers by Orthogonal Iterative Divergent/Convergent Approaches. *Macromolecular Rapid Communications* **2011,** *32* (2), 147-168.
39. Jiang, Y.; Golder, M. R.; Nguyen, H. V. T.; Wang, Y.; Zhong, M.; Barnes, J. C.; Ehrlich, D. J. C.; Johnson, J. A., Iterative Exponential Growth Synthesis and Assembly of Uniform Diblock Copolymers. *Journal of the American Chemical Society* **2016,** *138* (30), 9369-9372.
40. Barnes, J. C.; Ehrlich, D. J. C.; Gao, A. X.; Leibfarth, F. A.; Jiang, Y.; Zhou, E.; Jamison, T. F.; Johnson, J. A., Iterative exponential growth of stereo- and sequence-controlled polymers. *Nat Chem* **2015,** *7* (10), 810-815.
41. Leibfarth, F. A.; Johnson, J. A.; Jamison, T. F., Scalable synthesis of sequence-defined, unimolecular macromolecules by Flow-IEG. *Proceedings of the National Academy of Sciences* **2015,** *112* (34), 10617-10622.
42. Wicker, A. C.; Leibfarth, F. A.; Jamison, T. F., Flow-IEG enables programmable thermodynamic properties in sequence-defined unimolecular macromolecules. *Polymer Chemistry* **2017,** *8* (37), 5786-5794.
43. Huang, Z.; Zhao, J.; Wang, Z.; Meng, F.; Ding, K.; Pan, X.; Zhou, N.; Li, X.; Zhang, Z.; Zhu, X., Combining Orthogonal Chain-End Deprotections and Thiol–Maleimide Michael Coupling: Engineering Discrete Oligomers by an Iterative Growth Strategy. *Angewandte Chemie* **2017,** *129* (44), 13800-13805.

44. Delduc, P.; Tailhan, C.; Zard, S. Z., A convenient source of alkyl and acyl radicals. *Journal of the Chemical Society, Chemical Communications* **1988,** (4), 308-310.
45. Quiclet-Sire, B.; Zard, S., Z., Fun with radicals: Some new perspectives for organic synthesis. *Pure and Applied Chemistry* **2011,** *83* (3), 519-551.
46. Xu, J.; Shanmugam, S.; Fu, C.; Aguey-Zinsou, K.-F.; Boyer, C., Selective Photoactivation: From a Single Unit Monomer Insertion Reaction to Controlled Polymer Architectures. *Journal of the American Chemical Society* **2016,** *138* (9), 3094-3106.
47. Houshyar, S.; Keddie, D. J.; Moad, G.; Mulder, R. J.; Saubern, S.; Tsanaktsidis, J., The scope for synthesis of macro-RAFT agents by sequential insertion of single monomer units. *Polymer Chemistry* **2012,** *3* (7), 1879-1889.
48. Haven, J. J.; Vandenbergh, J.; Kurita, R.; Gruber, J.; Junkers, T., Efficiency assessment of single unit monomer insertion reactions for monomer sequence control: kinetic simulations and experimental observations. *Polymer Chemistry* **2015,** *6* (31), 5752-5765.
49. Xu, J.; Fu, C.; Shanmugam, S.; Hawker, C. J.; Moad, G.; Boyer, C., Synthesis of Discrete Oligomers by Sequential PET-RAFT Single-Unit Monomer Insertion. *Angewandte Chemie International Edition* **2017,** *56* (29), 8376-8383.
50. Annelore, A.; W., L. R.; Yanyan, Z.; Nino, M.; Graeme, M.; Almar, P., Light-Induced RAFT Single Unit Monomer Insertion in Aqueous Solution—Toward Sequence-Controlled Polymers. *Macromolecular Rapid Communications 0* (0), 1800240.
51. Porel, M.; Alabi, C. A., Sequence-Defined Polymers via Orthogonal Allyl Acrylamide Building Blocks. *Journal of the American Chemical Society* **2014,** *136* (38), 13162-13165.
52. Solleder, S. C.; Meier, M. A. R., Sequence Control in Polymer Chemistry through the Passerini Three-Component Reaction. *Angewandte Chemie International Edition* **2014,** *53* (3), 711-714.
53. Solleder, S. C.; Zengel, D.; Wetzel, K. S.; Meier, M. A. R., A Scalable and High-Yield Strategy for the Synthesis of Sequence-Defined Macromolecules. *Angewandte Chemie International Edition* **2016,** *55* (3), 1204-1207.
54. Zydziak, N.; Feist, F.; Huber, B.; Mueller, J. O.; Barner-Kowollik, C., Photo-induced sequence defined macromolecules via hetero bifunctional synthons. *Chemical Communications* **2015,** *51* (10), 1799-1802.
55. Zydziak, N.; Konrad, W.; Feist, F.; Afonin, S.; Weidner, S.; Barner-Kowollik, C., Coding and decoding libraries of sequence-defined functional copolymers synthesized via photoligation. *Nature Communications* **2016,** *7*, 13672.
56. Martens, S.; Van den Begin, J.; Madder, A.; Du Prez, F. E.; Espeel, P., Automated Synthesis of Monodisperse Oligomers, Featuring Sequence Control and Tailored Functionalization. *Journal of the American Chemical Society* **2016,** *138* (43), 14182-14185.
57. Martens, S.; Holloway, J. O.; Du Prez, F. E., Click and Click-Inspired Chemistry for the Design of Sequence-

Controlled Polymers. *Macromolecular Rapid Communications* **2017,** *38* (24), 1700469.

58. Waldemar, K.; R., B. F.; S., W. K.; C., B. A.; R., M. M. A.; Christopher, B. K., A Combined Photochemical and Multicomponent Reaction Approach to Precision Oligomers. *Chemistry – A European Journal* **2018,** *24* (14), 3413-3419.
59. König, N. F.; Telitel, S.; Poyer, S.; Charles, L.; Lutz, J. F., Photocontrolled Synthesis of Abiotic Sequence-Defined Oligo(Phosphodiester)s. *Macromolecular Rapid Communications* **2017,** *38* (24), 1700651.
60. Solleder, S. C.; Martens, S.; Espeel, P.; Du Prez, F.; Meier, M. A. R., Combining Two Methods of Sequence Definition in a Convergent Approach: Scalable Synthesis of Highly Defined and Multifunctionalized Macromolecules. *Chemistry – A European Journal* **2017,** *23* (56), 13906-13909.
61. Wu, Y.-H.; Zhang, J.; Du, F.-S.; Li, Z.-C., Dual Sequence Control of Uniform Macromolecules through Consecutive Single Addition by Selective Passerini Reaction. *ACS Macro Letters* **2017,** *6* (12), 1398-1403.
62. Cole, J. P.; Lessard, J. J.; Rodriguez, K. J.; Hanlon, A. M.; Reville, E. K.; Mancinelli, J. P.; Berda, E. B., Single-chain nanoparticles containing sequence-defined segments: using primary structure control to promote secondary and tertiary structures in synthetic protein mimics. *Polymer Chemistry* **2017,** *8* (38), 5829-5835.
63. Yu, L.; Zhang, Z.; You, Y.-Z.; Hong, C.-Y., Synthesis of sequence-controlled polymers via sequential thiol-ene and amino-yne click reactions in one pot. *European Polymer Journal* **2018,** *103*, 80-87.
64. Zhang, S.; Bauer, N. E.; Kanal, I. Y.; You, W.; Hutchison, G. R.; Meyer, T. Y., Sequence Effects in Donor–Acceptor Oligomeric Semiconductors Comprising Benzothiadiazole and Phenylenevinylene Monomers. *Macromolecules* **2017,** *50* (1), 151-161.
65. Zhang, S.; Hutchison, G. R.; Meyer, T. Y., Sequence Effects in Conjugated Donor–Acceptor Trimers and Polymers. *Macromolecular Rapid Communications* **2016,** *37* (11), 882-887.
66. Lawrence, J.; Lee, S.-H.; Abdilla, A.; Nothling, M. D.; Ren, J. M.; Knight, A. S.; Fleischmann, C.; Li, Y.; Abrams, A. S.; Schmidt, B. V. K. J.; Hawker, M. C.; Connal, L. A.; McGrath, A. J.; Clark, P. G.; Gutekunst, W. R.; Hawker, C. J., A Versatile and Scalable Strategy to Discrete Oligomers. *Journal of the American Chemical Society* **2016,** *138* (19), 6306-6310.
67. Lawrence, J.; Goto, E.; Ren, J. M.; McDearmon, B.; Kim, D. S.; Ochiai, Y.; Clark, P. G.; Laitar, D.; Higashihara, T.; Hawker, C. J., A Versatile and Efficient Strategy to Discrete Conjugated Oligomers. *Journal of the American Chemical Society* **2017,** *139* (39), 13735-13739.
68. Ren, J. M.; Lawrence, J.; Knight, A. S.; Abdilla, A.; Zerdan, R. B.; Levi, A. E.; Oschmann, B.; Gutekunst, W. R.; Lee, S.-H.; Li, Y.; McGrath, A. J.; Bates, C. M.; Qiao, G. G.; Hawker, C. J., Controlled Formation and Binding Selectivity of Discrete Oligo(methyl methacrylate) Stereocomplexes. *Journal of the American Chemical Society* **2018,** *140* (5), 1945-1951.
69. Vandenbergh, J.; Reekmans, G.; Adriaensens, P.; Junkers, T., Synthesis of sequence controlled acrylate oligomers

via consecutive RAFT monomer additions. *Chemical Communications* **2013,** *49* (88), 10358-10360.

70. Satoh, K.; Kamigaito, M., Stereospecific Living Radical Polymerization: Dual Control of Chain Length and Tacticity for Precision Polymer Synthesis. *Chemical Reviews* **2009,** *109* (11), 5120-5156.
71. Solleder, S. C.; Schneider, R. V.; Wetzel, K. S.; Boukis, A. C.; Meier, M. A. R., Recent Progress in the Design of Monodisperse, Sequence-Defined Macromolecules. *Macromolecular Rapid Communications* **2017,** *38* (9), 1600711.
72. Szymański, J. K.; Abul-Haija, Y. M.; Cronin, L., Exploring Strategies To Bias Sequence in Natural and Synthetic Oligomers and Polymers. *Accounts of Chemical Research* **2018,** *51* (3), 649-658.
73. Qu, C.; He, J., Recent developments in the synthesis of sequence controlled polymers. *Sci. China Chem.* **2015,** *58* (11), 1651-1662.
74. Natta, G.; Pino, P.; Corradini, P.; Danusso, F.; Mantica, E.; Mazzanti, G.; Moraglio, G., Crystalline High Polymer of α-Olefins. *Journal of the American Chemical Society* **1955,** *77* (6), 1708-1710.
75. Jiro, K.; Takehiro, K.; Kento, O.; Hiroshi, K.; Eiji, Y., Supramolecular Helical Structure of the Stereocomplex Composed of Complementary Isotactic and Syndiotactic Poly(methyl methacrylate)s as Revealed by Atomic Force Microscopy. *Angewandte Chemie International Edition* **2007,** *46* (28), 5348-5351.
76. Ming, R. J.; Kotaro, S.; Kit, G. T.; Anton, B.; Kanji, N.; Kenji, I.; Joseph, C. A.; George, Y.; Irene, Y.; Masami, K.; Guanghua, Q. G., Stereospecific Cyclic Poly(methyl methacrylate) and Its Topology-Guided Hierarchically Controlled Supramolecular Assemblies. *Angewandte Chemie International Edition* **2014,** *53* (2), 459-464.
77. Noble, B. B.; Coote, M. L., Chapter Four - Mechanistic Perspectives on Stereocontrol in Lewis Acid-Mediated Radical Polymerization: Lessons from Small-Molecule Synthesis. In *Advances in Physical Organic Chemistry*, Williams, I. H.; Williams, N. H., Eds. Academic Press: 2015; Vol. 49, pp 189-258.
78. Golder, M. R.; Jiang, Y.; Teichen, P. E.; Nguyen, H. V. T.; Wang, W.; Milos, N.; Freedman, S. A.; Willard, A. P.; Johnson, J. A., Stereochemical Sequence Dictates Unimolecular Diblock Copolymer Assembly. *Journal of the American Chemical Society* **2018,** *140* (5), 1596-1599.
79. Barnes, J. C.; Ehrlich, D. J. C.; Gao, A. X.; Leibfarth, F. A.; Jiang, Y.; Zhou, E.; Jamison, T. F.; Johnson, J. A., Iterative exponential growth of stereo- and sequence-controlled polymers. *Nature Chemistry* **2015,** *7*, 810.
80. Fu, C.; Huang, Z.; Hawker, C. J.; Moad, G.; Xu, J.; Boyer, C., RAFT-mediated, visible light-initiated single unit monomer insertion and its application in the synthesis of sequence-defined polymers. *Polymer Chemistry* **2017,** *8* (32), 4637-4643.
81. Braun, D.; Hu, F., Polymers from non-homopolymerizable monomers by free radical processes. *Progress in Polymer Science* **2006,** *31* (3), 239-276.
82. Mokhtar, S. M.; Mikhael, M. G.; Aly, R. O.; Elsabee, M. Z., Copolymerization of Indene with N-Phenylmaleimide. *Polymer Journal* **1988,** *20*, 979.

83. Xu, J.; Jung, K.; Atme, A.; Shanmugam, S.; Boyer, C., A Robust and Versatile Photoinduced Living Polymerization of Conjugated and Unconjugated Monomers and Its Oxygen Tolerance. *Journal of the American Chemical Society* **2014,** *136* (14), 5508-5519.
84. Phommalysack-Lovan, J.; Chu, Y.; Boyer, C.; Xu, J., PET-RAFT polymerisation: towards green and precision polymer manufacturing. *Chemical Communications* **2018,** *54* (50), 6591-6606.
85. Shanmugam, S.; Xu, J.; Boyer, C., Exploiting Metalloporphyrins for Selective Living Radical Polymerization Tunable over Visible Wavelengths. *Journal of the American Chemical Society* **2015,** *137* (28), 9174-9185.
86. Stenzel, M. H.; Davis, T. P., Star polymer synthesis using trithiocarbonate functional β-cyclodextrin cores (reversible addition–fragmentation chain-transfer polymerization). *Journal of Polymer Science Part A: Polymer Chemistry* **2002,** *40* (24), 4498-4512.
87. Xu, J.; Jung, K.; Boyer, C., Oxygen Tolerance Study of Photoinduced Electron Transfer–Reversible Addition–Fragmentation Chain Transfer (PET-RAFT) Polymerization Mediated by Ru(bpy)3Cl2. *Macromolecules* **2014,** *47* (13), 4217-4229.
88. Cubbon, R. C. P., Preparation of Alternating Copolymers of the N-Substituted Maleimides. *Journal of Polymer Science Part C: Polymer Symposia* **1967,** *16* (1), 387-392.
89. Oishi, T.; Yamasaki, H.; Fujimoto, M., Asymmetric Polymerization of N-Substituted Maleimide. *Polymer Journal* **1991,** *23*, 795.
90. Liu, W.; Chen, C.; Chen, Y.; Xi, F., Asymmetric polymerization of N-triphenylmethylmaleimide with chiral anionic initiators. *Polymer Bulletin* **1997,** *38* (5), 509-514.
91. Cubbon, R. C. P., The free radical and anionic polymerization of some N-substituted maleimides. *Polymer* **1965,** *6* (8), 419-426.
92. Ha, N. T. H.; Fujimori, K.; Tucker, D. J., Monomer unit sequence distribution and linkage configurations at citraconic anhydride units in the copolymers of citraconic anhydride and styrene prepared in carbon tetrachloride. *Polymer Bulletin* **1997,** *38* (5), 569-572.
93. Quiclet-Sire, B.; Revol, G.; Zard, S. Z., A convergent, modular access to complex amines. *Tetrahedron* **2010,** *66* (33), 6656-6666.

Graphic Abstract